

**A peer-reviewed version of this preprint was published in PeerJ on 10 July 2014.**

[View the peer-reviewed version](https://doi.org/10.7717/peerj.470) (peerj.com/articles/470), which is the preferred citable publication unless you specifically need to cite this preprint.

Bernardo CEP, Silva PJ. 2014. Computational development of rubromycin-based lead compounds for HIV-1 reverse transcriptase inhibition. PeerJ 2:e470 <https://doi.org/10.7717/peerj.470>

# Computational development of rubromycin-based lead compounds for HIV-1 reverse transcriptase inhibition

The binding of several rubromycin-based ligands to HIV1-reverse transcriptase was analyzed using molecular docking and molecular dynamics simulations. MM-PBSA analysis and examination of the trajectories allowed the identification of several promising compounds with predicted high affinity towards reverse transcriptase mutants which have proven resistant to current drugs. Important insights on the complex interplay of factors determining the ability of ligands to selectively target each mutant have been obtained.

# Computational development of rubromycin-based lead compounds for HIV-1 reverse transcriptase inhibition

*Carlos E. P. Bernardo and Pedro J. Silva\**

*REQUIMTE/Faculdade de Ciências da Saúde, Universidade Fernando Pessoa, Rua*

*Carlos da Maia, 296, 4200-150 Porto, Portugal*

## Abstract

The binding of several rubromycin-based ligands to HIV1-reverse transcriptase was analyzed using molecular docking and molecular dynamics simulations. MM-PBSA analysis and examination of the trajectories allowed the identification of several promising compounds with predicted high affinity towards reverse transcriptase mutants which have proven resistant to current drugs. Important insights on the complex interplay of factors determining the ability of ligands to selectively target each mutant have been obtained.

## Introduction

HIV reverse transcriptases are multifunctional enzymes which use the virus single-stranded RNA genome as template to build a double-stranded DNA which may later be incorporated into the host's genome. They are composed of two subunits: p66 acts both as a DNA polymerase and as a RNAase which cleaves RNA/DNA hybrid molecules and p51 (whose sequence is equal to that of p66, but lacks the last 124 aminoacids) plays mostly a structural role. Due to its crucial role in the virus life cycle, HIV reverse transcriptase (RT) has been the target of several successful drug-developing efforts. These drugs may be grouped in several classes based on their mechanism of action (thoroughly reviewed in(Jochmans, 2008; Sarafianos et al., 2009; Singh et al., 2010)): nucleoside analogue RT inhibitor (NRTI), like azidothymidine(Mitsuya et al., 1985) (the first successful drug against HIV) act as a alternative substrates and block the synthesis of the viral DNA due to their lack of a free 3' OH- group; nucleotide-competing RT inhibitors (NcRTI) like INDOPY-1(Jochmans et al., 2006) bind the active site in an as-yet-undisclosed manner; and non-nucleoside RT inhibitors (NNRTI) in contrast bind to the enzyme in a hydrophobic pocket 10 Å away from the active site(Kohlstaedt et al., 1992; Ding et al., 1998) and prevent the enzyme from attaining a catalytically competent conformation. Since reverse transcriptases lack a proofreading ability, very high rates of mutation are observed and mutants resistant to one or more drugs frequently arise. To decrease the probability of selection of drug-resistant strains, a combination therapy including drugs with different targets and modes of action is most often used in clinical practice. Still, newer drugs must be continually developed to fight resistant strains.

Rubromycins are a small class of compounds containing naphthoquinone and 8-hydroxyisocoumarin moieties (Brasholz et al., 2007). In 1990,  $\beta$ - and  $\gamma$ -rubromycin were shown to inhibit HIV-1 reverse transcriptase (Goldman et al., 1990), although at levels that were also toxic to human T lymphocytes.  $\gamma$ -rubromycin was later shown to be an inhibitor of human telomerase (Ueno et al., 2000), fueling interest in its use as an anti-cancer agent. The development of less toxic variants of these lead compounds has long been prevented due to the difficulty of their laboratory synthesis, but several synthetic routes to these interesting molecules have recently become available (Akai et al., 2007; Rathwell et al., 2009; Wu, Mercado, & Pettus, 2011), enabling the evaluation of many derivatives as candidates for the inhibition of telomerase (Yuen et al., 2013). In this report, we describe the evaluation of rubromycin derivatives as inhibitors of HIV-1 reverse transcriptase using computational docking and molecular dynamics simulations of the most promising candidates. The results are compared to those of the commercially-available, 2<sup>nd</sup>-generation NNRTI drug rilpivirine.

### Computational methods

All computations were performed in YASARA (Krieger et al., 2004) using the crystal structure of the rilpivirine-inhibited HIV1 reverse transcriptase published by Das *et al.* (PDB: 2ZD1) (Das et al., 2008). A double-mutant structure, (p66)K103N/(p66)Y181C and a quadruple mutant (p51p66)M184I/(p51p66)E138K, were also generated to evaluate the robustness of the ligand binding to reverse transcriptase variants with increased resistance to NNRTIs: K103N is known to strongly reduce susceptibility to efavirenz and nevirapine (Bachelier et al., 2001; Rhee et al., 2004; Eshleman et al., 2006; Zhang et al., 2007; Melikian et al., 2014) and E138K has a similar effect towards

rilpivirine, which is increased by M184I(Kulkarni et al., 2012); Y181C reduces susceptibility to efavirenz, etravirine and rilpivirine(Reuman et al., 2010; Tambuyzer et al., 2010; Rimsky et al., 2012). Rubromycin-based ligands (Figure 1 and Supporting Information) were docked to the wild-type structure with AutoDock 4.2.3(Morris et al., 2009) using default docking parameters and point charges assigned according to the AMBER03 force field(Duan et al., 2003). The highest scoring ligands and poses were selected for molecular dynamics simulations. Initial structures for molecular dynamics simulations of mutant proteins were generated from the corresponding ligand-bound wild-type structures through mutation of the corresponding aminoacids. All simulations were run with the AMBER03 forcefield(Duan et al., 2003), using a multiple time step of 1.25 fs for intramolecular and 2.5 fs for intermolecular forces. Simulations were performed in cells 5 Å larger than the solute along each axis (final cell dimensions  $127.3 \times 102.6 \times 78.8$  Å), and counter-ions (88 Cl<sup>-</sup> and 77 Na<sup>+</sup>) were added to a final concentration of 0.9 % NaCl. In total, the simulation contained approximately 106,500 atoms. A 7.86 Å cutoff was taken for Lennard-Jones forces and the direct space portion of the electrostatic forces, which were calculated using the Particle Mesh Ewald method(Essmann et al., 1995) with a grid spacing <1 Å, 4th order B-splines and a tolerance of  $10^{-4}$  for the direct space sum. Simulated annealing minimizations started at 298 K, velocities were scaled down with 0.9 every ten steps for a total time of 5 ps. After annealing, simulations were run at 298 K. Temperature was adjusted using a Berendsen thermostat(Berendsen et al., 1984) based on the time-averaged temperature, i.e., to minimize the impact of temperature control, velocities were rescaled only about every 100 simulation steps, whenever the average of the last 100 measured temperatures converged. Substrate parameterization was performed with the AM1BCC protocol(Jakalian et al., 2000; Jakalian, Jack, & Bayly, 2002). All simulations were run

for 30 ns. Differences in ligand binding energies between wild-type and mutant proteins were evaluated using the MM-PBSA methodology(Srinivasan et al., 1998): for each snapshot (taken at 0.25 ns intervals from the last 15 ns of the simulation) we computed the molecular mechanics energy of the protein-ligand complex, the electrostatic contribution to solvation energy (using the Adaptive Poisson-Boltzmann Solver (Baker et al., 2001)) and nonelectrostatic contributions to solvation (with a surface-area-dependent term(Wang et al., 2001)). These computations were repeated for each snapshot for the ligand-free protein and the protein-free ligad, to obtain an estimate of the average binding energy of each ligand.

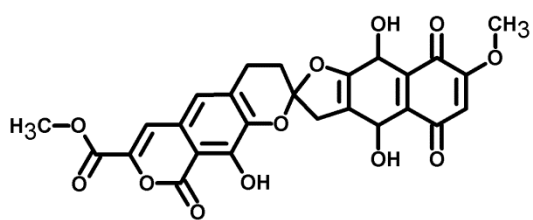
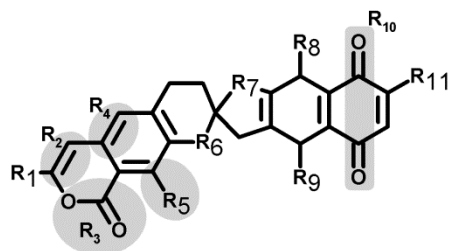
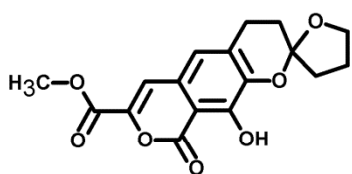
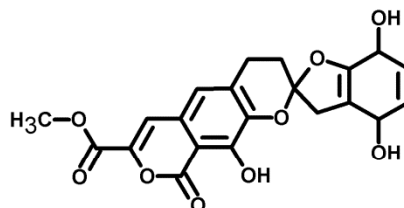
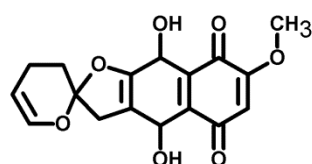
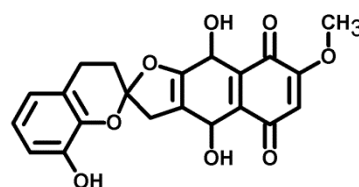
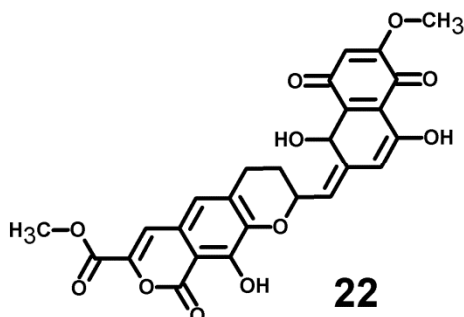
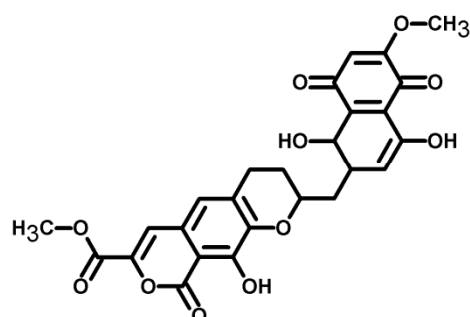
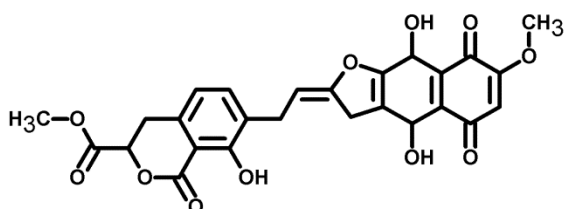
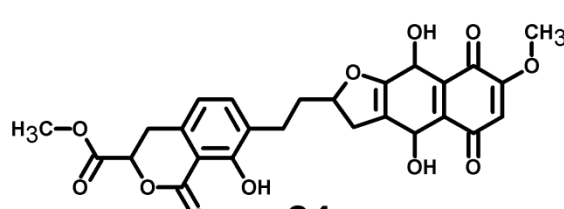
**rubromycin****1-14 ; 17 ; 20-21 ; 26-46****15****16****18****19****22****25****23****24**

Figure 1: Structures of the tested rubromycin-based ligands.



### III. Results

Table 1: Substitution patterns and AutoDock-computed binding energies of the best-scoring ligands. Only differences from the parent compound ( $\gamma$ -rubromycin) are shown. The binding energy of the drug rilpivirine, computed with the same methods, amounts to  $-13.25 \text{ kcal.mol}^{-1}$ . Data for all ligands is available as Supporting Information.

Ligand:	<b>Rubromycin</b>	<b>46</b>	<b>36</b>	<b>27</b>	<b>45</b>	<b>13</b>	<b>38</b>	<b>37</b>
R <sub>1</sub> =	-COOCH <sub>3</sub>				-CH <sub>2</sub> OH			
R <sub>2</sub> =	-C=C-H			(S) HC-CH <sub>2</sub>				
R <sub>3</sub> =	-C=O-O				-O-C=O			
R <sub>4</sub> =	=C=C-H	-CH-CH <sub>2</sub> -						
R <sub>5</sub> =	-C-OH	-C=O						
R <sub>6</sub> =	-O-							
R <sub>7</sub> =	-O-							
R <sub>8</sub> =	-OH							
R <sub>9</sub> =	-OH							
R <sub>10</sub> =	-C=O -C=O							
R <sub>11</sub> =	-O-CH <sub>3</sub>	-CN	-F		-CN	-CH <sub>2</sub> -CH <sub>3</sub>	-CN	-Cl
Binding energy	-12.95	-13.71	-13.72	-13.82	-13.82	-13.91	-14.25	-14.29

Computational docking allows the fast screening of a large number of candidate ligands, which may afterwards be analyzed through more demanding computational techniques in the search for suitable leads for further development and experimental characterization. Our initial screen analyzed the docking performance of rubromycin derivatives with/without truncated rings, substitution of the oxygen atoms appended to the spirocyclic ring and different substitution patterns around the rings. The worst-scoring ligands were those where any of the rings had been removed, as well as the ones

where the oxygen at the R<sub>6</sub> position was substituted by nitrogen or carbon. Surprisingly, substitution of the =CH- at the R<sub>4</sub> position by an isoelectronic =N- also led to a dramatic loss of binding affinity. The most promising leads (Table 1) generally had (like the NNRTI drug rilpivirine) a nitrile group appended to the ligand. The behavior of these molecules in the reverse transcriptase binding pocket of wild-type and mutant reverse transcriptase was then evaluated through 30 ns-long molecular dynamics simulations and compared to that of rilpivirine.

Table 2: Binding affinity (average  $\pm$  standard error of the mean) of the best-scoring ligands to reverse-transcriptase mutants, relative to the binding affinity of each ligand to the wild-type enzyme. Values in kcal.mol<sup>-1</sup>. Negative values show stronger binding than observed to the wild-type protein.

	<b>K103N / Y181C</b>	<b>E138 K / M184I</b>
<b>Rilpivirine</b>	1.6 $\pm$ 0.9	3.6 $\pm$ 0.8
<b><math>\gamma</math>-rubromycin</b>	9.8 $\pm$ 1.1	0.3 $\pm$ 1.1
<b>13</b>	-6.7 $\pm$ 1.4	-16.8 $\pm$ 1.4
<b>27</b>	7.7 $\pm$ 1.4	-13.0 $\pm$ 1.2
<b>36</b>	10.3 $\pm$ 1.0	-7.1 $\pm$ 0.9
<b>37</b>	-4.0 $\pm$ 1.2	-5.2 $\pm$ 1.4
<b>38</b>	4.6 $\pm$ 1.0	-4.1 $\pm$ 0.9
<b>45</b>	-3.6 $\pm$ 1.0	-7.0 $\pm$ 1.2
<b>46</b>	-1.9 $\pm$ 1.2	-3.8 $\pm$ 1.0

Binding affinities of each ligand to wild-type and mutant HIV-1 RT s were computed with the MM-PBSA methodology using the last 15 ns of each molecular dynamics simulation (Table 2). This method, while not accurate enough to produce reliable absolute binding free energies, has been shown to provide good estimates of binding affinity trends provided that either the ligands or the protein targets under comparison are very similar (Massova & Kollman, 2000). The computed data for rilpivirine agree with the experimentally observed sensitivity of its binding to E138K / M184I variants, and to the relative insensitivity of its effect on the presence/absence of K103N or Y181C mutation, which supports the applicability of the MM-PBSA approach to this system. Ligands **13**, **27**, **36** and **45** are computed to bind significantly stronger to the rilpivirine-resistant E138K/M184I HIV1-RT variant than to the wild-type protein, and may therefore be suitable lead compounds for further pharmaceutical developments against rilpivirine-resistant strains. Further insight to the determinants of binding affinity was obtained through close inspection of each simulation.

As observed in the crystal structure(Das et al., 2008), rilpivirine remains bound to RT throughout the simulation through a large number of hydrophobic contacts and two very stable hydrogen bonds with the backbone of Lys101, whether in the wild-type or any of the tested mutants. Its high hydrophobicity strongly favor it to adopt a very buried conformation and low solvent-accessible area throughout the simulation. The high stability of the hydrogen bonds does not change in the mutated variants, but the total number of close hydrophobic contacts between rilpivirine and the protein does become smaller in the E138K/M184I mutant, which is consistent with the experimentally observed lower affinity of this drug towards it (Singh et al., 2012), and the computed MM-PBSA binding energy.

$\gamma$ -rubromycin is a much larger and less flexible ligand than rilpivirine: as it binds to the NNRTI binding patch, the methoxy-bearing end of  $\gamma$ -rubromycin remains in contact with the solvent through its hydrophilic surface (Figure 2), whereas the oxygen atoms in its naphthoquinone moiety establish stable hydrogen bonds with Lys101 and Lys103. In the K103N/Y181C mutant,  $\gamma$ -rubromycin becomes less exposed to the solvent, since the shorter sidechain of Asn103 (compared to the wild-type Lys 103) forces the naphthoquinone moiety of the ligand to penetrate deeper into the crevice in order to establish a stabilizing hydrogen bond with Asn103. The buried conformation of  $\gamma$ -rubromycin removes the methoxy group from its favored solvent-exposed environment leading to a binding mode which is computed by MM-PBSA to be markedly less favored than observed in the wild-type protein, but which remains stable due to the difficulty in breaking the large number of favorable hydrogen bonds to Asn103 and Lys101.  $\gamma$ -rubromycin binding to the E138K/M184I is very similar to the wild-type protein: hydrogen bonds between the ligand and Lys101 and Lys103 are also present (though ca. 0.4 Å longer), and subtle cavity rearrangements due to the loss of the ionic bridge between Lys101 and (p51)Glu138 (which is mutated to a Lys) lead to the possibility of intermittent H-bonded interactions between the carbonyl of Ile180 (or the sidechain of (p51)Thr139) and the naphthoquinone moiety.

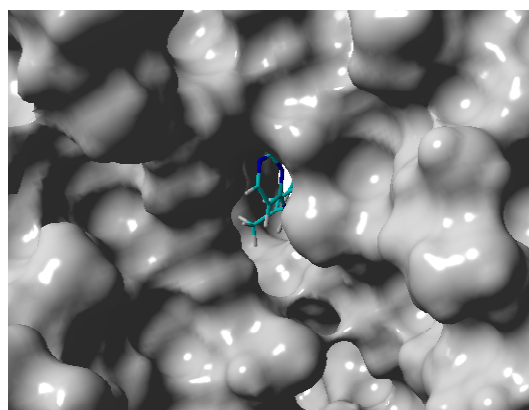
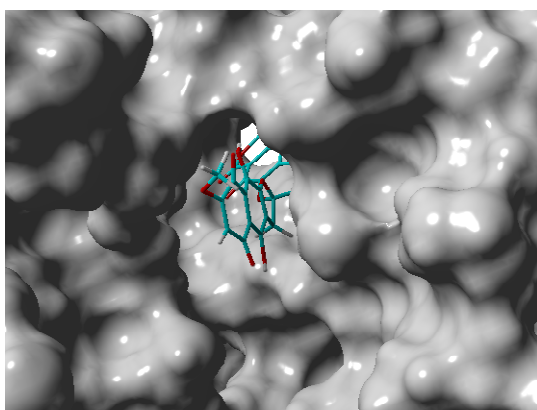


Figure 2:  $\gamma$ -rubromycin (left panel) and rilpivirine (right panel) bound to wild-type HIV-1 reverse transcriptase. Snapshots were taken from random points in the last 15ns of molecular dynamics simulations.

The binding of ligand **13** to wild type RT differs more from that of  $\gamma$ -rubromycin than would be expected from the very small difference in their structures (the single substitution of a methoxy group in  $\gamma$ -rubromycin by an ethyl): since the ethyl group is less hydrophilic than a methoxy, it initially tends to establish a hydrophobic interaction with the sidechain of Val179, instead of protruding (like the methoxy group) in the direction of the solvent, leading to a binding mode where the stabilizing hydrogen-bonds between the ligand and the protein are due to Glu138 instead of Lys101. In contrast to what is observed in the binding of  $\gamma$ -rubromycin to the K103N/Y181C, the replacement of the Lys-based H-bonds does not lead to an unfavorable buried conformation of the ligand because, as the simulation progresses, the interaction with Glu138 causes subtle changes in the local environment which becomes more exposed to the solvent than originally: indeed, there is in average one more water molecule near ligand **13** than near  $\gamma$ -rubromycin, leading to a smaller desolvation penalty when **13** binds to the protein. Binding of **13** to the mutants is strongly favored over binding to the wild-type due to the formation of hydrogen bonding to the backbone of Ile180 (especially in E138K/M184I) and especially by the changes in the electrostatic component of ligand solvation caused by the presence of two intra-molecular H-bonds in **13** when bound to the mutant proteins.

The  $sp^3$  hybridization in the acetyl-bearing carbon of the isocoumarin-moiety in **27** introduces a deviation from full planarity in that region of the ligand, which facilitates its interactions with the Trp229 and Ty188 aminoacids on that end of the NNRTI-

binding cavity. Ligand **27** is found to bind much more favorably to the quadruple mutant E138K/M184I (with a very large number of very short and stable hydrogen bonds with Lys101, Lys103, Lys138 and Thr139) than to wild-type or K103N/Y181C, where the only stable hydrogen bonds available are those with Glu138. The electrostatic component of the solvation energy of **27** follows the opposite trend as the protein is changed from WT to the mutants, but the smaller variation of this factor simply dampens the magnitude of the change in binding affinities brought about by the variation in protein-ligand interactions.

Ligand **36** bears a fluorine atom in place of the methoxy group carried by  $\gamma$ -rubromycin. Like ligand **27**, **36** has higher affinity to the E138K/M184I mutant than to either the wild-type and, especially, the K103N/Y181C mutant. The minute size of the fluorine substituent allows Lys101 and Glu138 (which lie on opposite sides of the crevice where the ligands bind) to approach each other and form a strong ionic bridge which pushes the ligand further inside the cavity. This ionic bridge cannot form in the E138K/M184I mutant, leading to a binding mode where the ligand is slightly more exposed and strongly binds to Lys101, Lys103 and Lys 138. In the K103N/Y181C, the interactions between ligand and protein are weaker due to the strong deviations from 180° in the possible H-bonding partners in the binding cavity.

Ligands **37** and **38** bear a chlorine and a cyanide (respectively) in place of the fluorine present on **36**. The intermediate size of these substituents (relative to the fluorine in **36** and the methoxy in  $\gamma$ -rubromycin) leads to an intermediate degree of penetration in the binding cavity, between those of **36** and in  $\gamma$ -rubromycin. As observed in most cases, Lys101 is responsible for the most stable interaction between protein and ligand. No single contribution is, however, determinant in the observed trend of binding affinity of **37** to the proteins, as the correlation of total binding energies to either electrostatic

components of solvation or to protein-ligand interaction is insignificant: the overall effect is rather the result of subtle interplay of the electrostatic component of solvation and the protein-ligand interaction. Solvation effects, in contrast are determinant in the binding trends observed for ligand **38**, as the higher affinity to the M184I/E138K mutant is correlated to its much smaller desolvation penalty, which is due to the considerable exposure of its nitrile group to solvent when the entrance to the binding channel is not blocked by the Glu138-Lys101 ionic bond (Fig.3).

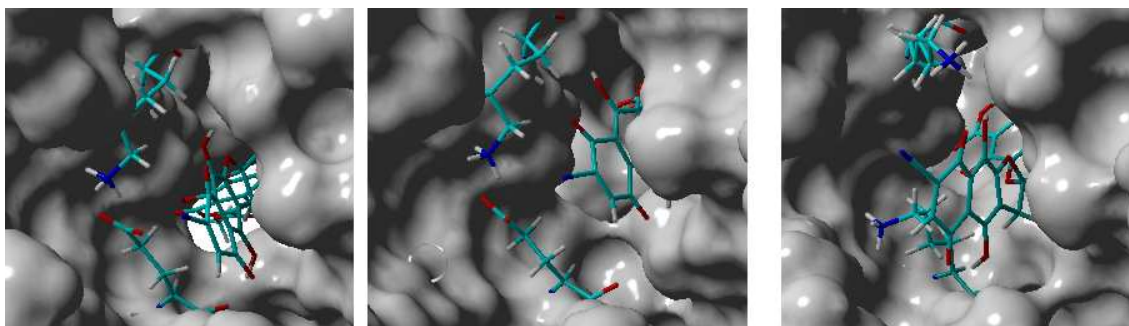


Figure 3: Ligand **38** bound to wild-type (left panel), K103N/Y181C (center panel) and E138K/M184I (right panel). Snapshots were taken from random points in the last 15ns of molecular dynamics simulations.

Ligand **45** bears, like ligands **38** and **46**, a nitrile group in the position occupied by a methoxy in  $\gamma$ -rubromycin. It differs from **38** by the replacement of the acetyl substituent of the isocoumarin by a hydroxymethyl and by switching the orientation of the lactone group in isocoumarin from  $-O-C=O$  to  $O=C-O$ . The replacement of acetyl from hydroxymethyl makes the isocoumarin end of **45** significantly smaller and less hydrophilic, leading that end of the molecule towards the inside of the crevice and the nitrile-bearing naphthoquinone portion of **45** to protrude from the other end of the cavity into the solvent (Figure 4). The only H-bonds between ligand and protein now involve

the backbone atoms of Lys101 and Glu138. These H-bonds weaken considerably in both mutants, but this destabilizing effect is overtaken by sizable stabilizing effects due to favorable solvation, leading to overall better binding to K103N/Y181C and (especially) E138K/M184I.

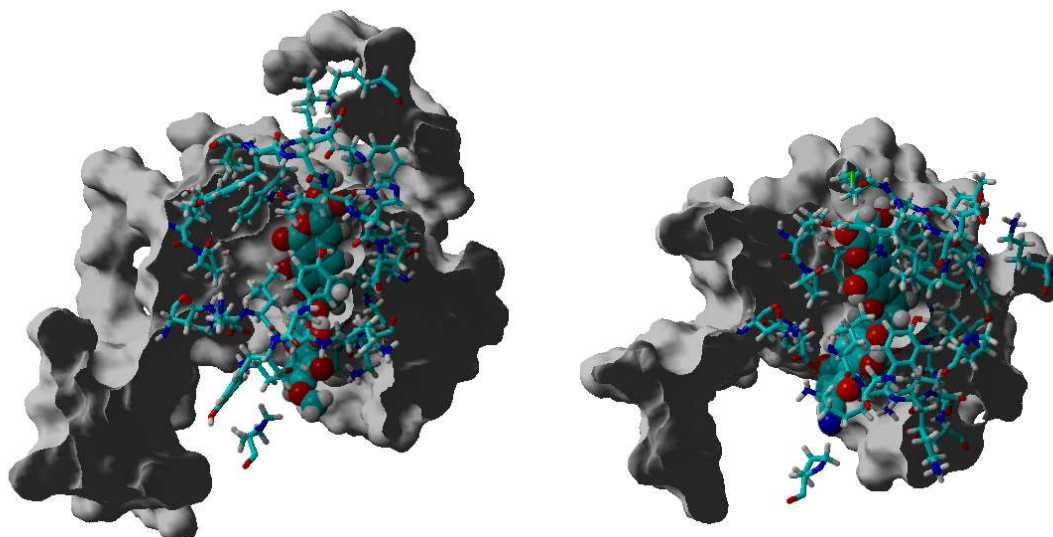


Figure 4: NNRTI-binding channel in wild-type reverse transcriptase filled with  $\gamma$ -rubromycin (left panel or ligand **47**(right panel). Only aminoacids within 13 Å from the ligand are shown. Ligand atoms are shown as spheres. The isocoumarin end of the ligand is oriented towards the top of the image and the naphthoquinone moiety towards the bottom.

Other than the lack of H-bond donating ability in its isocoumarin moiety (due to the replacement of its hydroxyl by a carbonyl), ligand **46** is identical to ligand **38**. Unlike ligand **38**, its ability to bind the K103N/Y181C mutant is not inferior to its affinity to the wild-type protein: the presence of a carbonyl instead of a hydroxyl allows it to accept a hydrogen bond from Tyr183, which is able to rotate into position in the mutant due to the smaller size occupied by Cys181 (compared to the original tyrosine present in the wild type).



## Influence of ligand binding on protein dynamics

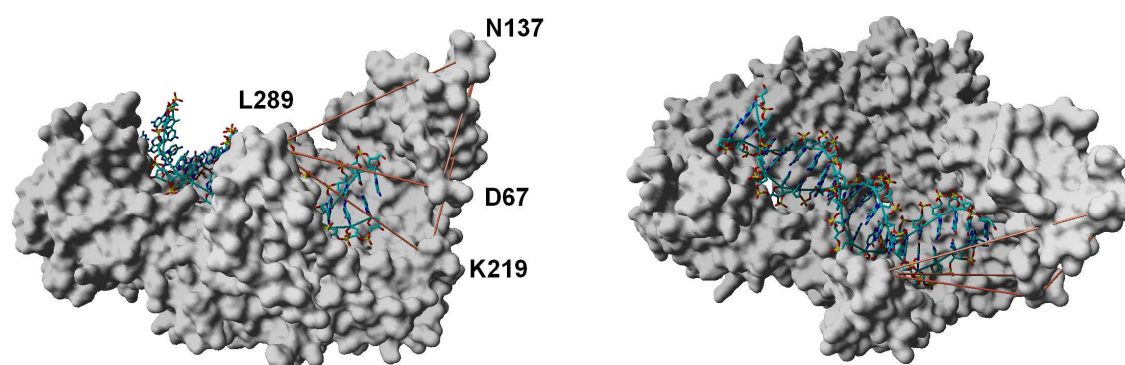


Figure 5: Structure of nucleic acid-bound reverse transcriptase. Distances between the shown aminoacids were used as “fingerprints” for the identification of catalytically competent conformations

In the absence of NNRTI, reverse transcriptase may adopt either a compact structure(Hsiou et al., 1996) or an open structure (Ding et al., 1998) which allows the binding of a RNA template and the polymerization of DNA. The binding of a NNRTI acts as a “wedge”(Ivetac & McCammon, 2009) that further separates the catalytic triad (Asp110, Asp185 and Asp186) from Met230, which is believed to be part of the primer-recognition region. Through distance analysis of our simulations confirms that the same “wedge” effect is observed for the tested ligands (Figure 6).

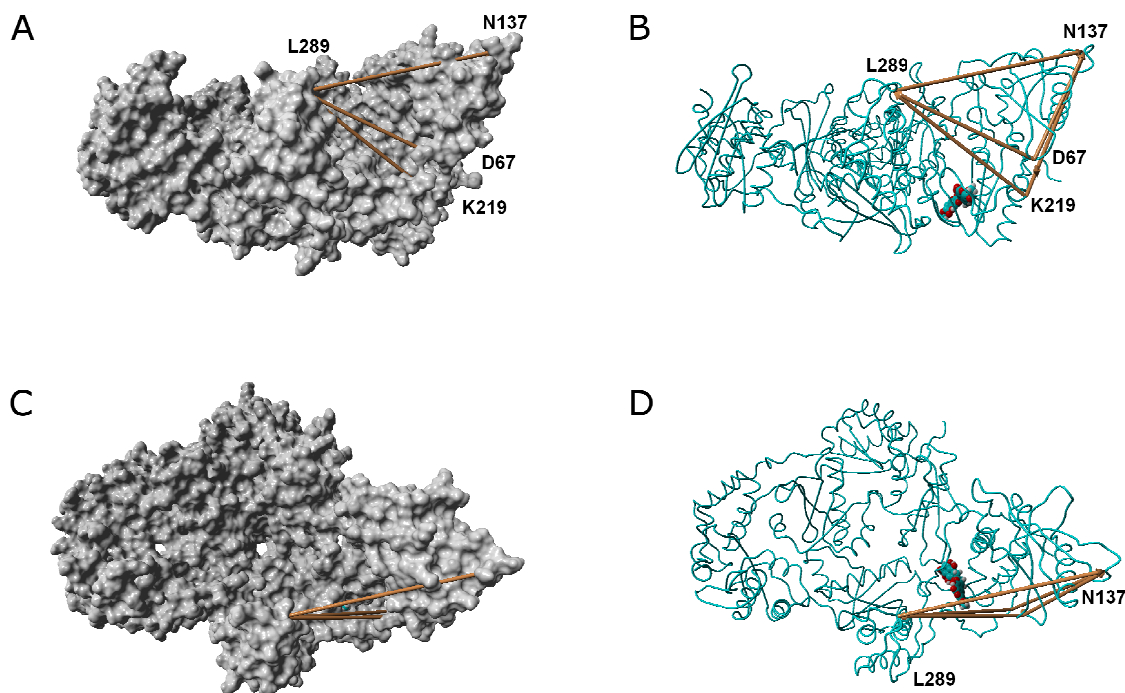


Figure 6: Representative structure of ligand-bound reverse transcriptase. Distances between the shown aminoacids were used as “fingerprints” for the search of catalytically competent conformations. Panels A and B: “side view”. Panels C and D: “top” view.

## Conclusions

Our computational study confirms that rubromycin-based ligands are able to bind to HIV1-reverse transcriptase at the previously defined NNRTI-binding site, and allowed the identification of ligands that are predicted to bind very strongly to RT mutants which have shown high resistance towards other NNRTI compounds. The best compounds (**13**, **27**, **36** and **45**) achieve selective binding to the highly resistant mutant E138K/M184I through very subtle variations on the degree of exposure to solvent, and on the number and strength of hydrogen bonds and hydrophobic interactions with the protein.

## References

- Akai, S., Kakiguchi, K., Nakamura, Y., Kuriwaki, I., Dohi, T., Harada, S., Kubo, O., Morita, N., & Kita, Y. 2007. *Total synthesis of (+/-)-gamma-rubromycin on the basis of two aromatic Pummerer-type reactions*. *Angewandte Chemie (International ed. in English)* 46(39):7458–61.
- Bachelor, L., Jeffrey, S., Hanna, G., D'Aquila, R., Wallace, L., Logue, K., Cordova, B., Hertogs, K., Larder, B., Buckery, R., et al. 2001. *Genotypic correlates of phenotypic resistance to efavirenz in virus isolates from patients failing nonnucleoside reverse transcriptase inhibitor therapy*. *Journal of virology* 75(11):4999–5008.
- Baker, N. A., Sept, D., Joseph, S., Holst, M. J., & McCammon, J. A. 2001. *Electrostatics of nanosystems: application to microtubules and the ribosome*. *Proceedings of the National Academy of Sciences of the United States of America* 98(18):10037–41.
- Berendsen, H. J. C., Postma, J. P. M., van Gunsteren, W. F., DiNola, A., & Haak, J. R. 1984. *Molecular dynamics with coupling to an external bath*. *The Journal of Chemical Physics* 81(8):3684.
- Brasholz, M., Sörgel, S., Azap, C., & Reißig, H.-U. 2007. *Rubromycins: Structurally Intriguing, Biologically Valuable, Synthetically Challenging Antitumour Antibiotics*. *European Journal of Organic Chemistry* 2007(23):3801–3814.
- Das, K., Bauman, J. D., Clark, A. D., Frenkel, Y. V, Lewi, P. J., Shatkin, A. J., Hughes, S. H., & Arnold, E. 2008. *High-resolution structures of HIV-1 reverse transcriptase/TMC278 complexes: strategic flexibility explains potency against resistance mutations*. *Proceedings of the National Academy of Sciences of the United States of America* 105(5):1466–71.
- Ding, J., Das, K., Hsiou, Y., Sarafianos, S. G., Clark, A. D., Jacobo-Molina, A., Tantillo, C., Hughes, S. H., & Arnold, E. 1998. *Structure and functional implications of the polymerase active site region in a complex of HIV-1 RT with a double-stranded DNA template-primer and an antibody Fab fragment at 2.8 Å resolution*. *Journal of molecular biology* 284(4):1095–111.
- Duan, Y., Wu, C., Chowdhury, S., Lee, M. C., Xiong, G., Zhang, W., Yang, R., Cieplak, P., Luo, R., Lee, T., et al. 2003. *A point-charge force field for molecular mechanics simulations of proteins based on condensed-phase quantum mechanical calculations*. *Journal of computational chemistry* 24(16):1999–2012.
- Eshleman, S. H., Jones, D., Galovich, J., Paxinos, E. E., Petropoulos, C. J., Jackson, J. B., & Parkin, N. 2006. *Phenotypic drug resistance patterns in subtype A HIV-1 clones with nonnucleoside reverse transcriptase resistance mutations*. *AIDS research and human retroviruses* 22(3):289–93.
- Essmann, U., Perera, L., Berkowitz, M. L., Darden, T., Lee, H., & Pedersen, L. G. 1995. *A smooth particle mesh Ewald method*. *The Journal of Chemical Physics* 103(19):8577.

Goldman, M., Salituro, G., Bowen, J., Williamson, J., Zink, D., Schleif, W., & Emini, E. 1990. *Inhibition of human immunodeficiency virus-1 reverse transcriptase activity by rubromycins: competitive interaction at the template.primer site*. *Mol. Pharmacol.* 38(1):20–25.

Hsiou, Y., Ding, J., Das, K., Clark, A. D., Hughes, S. H., & Arnold, E. 1996. *Structure of unliganded HIV-1 reverse transcriptase at 2.7 Å resolution: implications of conformational changes for polymerization and inhibition mechanisms*. *Structure (London, England)*: 1993) 4(7):853–60.

Ivetac, A., & McCammon, J. A. 2009. *Elucidating the inhibition mechanism of HIV-1 non-nucleoside reverse transcriptase inhibitors through multicopy molecular dynamics simulations*. *Journal of molecular biology* 388(3):644–58.

Jakalian, A., Bush, B. L., Jack, D. B., & Bayly, C. I. 2000. *Fast, efficient generation of high-quality atomic charges. AM1-BCC model: I. Method*. *Journal of Computational Chemistry* 21(2):132–146.

Jakalian, A., Jack, D. B., & Bayly, C. I. 2002. *Fast, efficient generation of high-quality atomic charges. AM1-BCC model: II. Parameterization and validation*. *Journal of Computational Chemistry* 23(16):1623–1641.

Jochmans, D. 2008. *Novel HIV-1 reverse transcriptase inhibitors*. *Virus research* 134(1-2):171–85.

Jochmans, D., Deval, J., Kesteleyn, B., Van Marck, H., Bettens, E., De Baere, I., Dehertogh, P., Ivens, T., Van Ginderen, M., Van Schoubroeck, B., et al. 2006. *Indolopyridones inhibit human immunodeficiency virus reverse transcriptase with a novel mechanism of action*. *Journal of virology* 80(24):12283–92.

Kohlstaedt, L. A., Wang, J., Friedman, J. M., Rice, P. A., & Steitz, T. A. 1992. *Crystal structure at 3.5 Å resolution of HIV-1 reverse transcriptase complexed with an inhibitor*. *Science (New York, N.Y.)* 256(5065):1783–90.

Krieger, E., Darden, T., Nabuurs, S. B., Finkelstein, A., & Vriend, G. 2004. *Making optimal use of empirical energy functions: Force-field parameterization in crystal space*. *Proteins-Structure Function and Bioinformatics* 57:678–683.

Kulkarni, R., Babaoglu, K., Lansdon, E. B., Rimsky, L., Van Eygen, V., Picchio, G., Svarovskaia, E., Miller, M. D., & White, K. L. 2012. *The HIV-1 reverse transcriptase M184I mutation enhances the E138K-associated resistance to rilpivirine and decreases viral fitness*. *Journal of acquired immune deficiency syndromes (1999)* 59(1):47–54.

Massova, I., & Kollman, P. A. 2000. *Combined molecular mechanical and continuum solvent approach (MM-PBSA/GBSA) to predict ligand binding*. *Perspectives in Drug Discovery and Design* 18(1):113–135.

Melikian, G. L., Rhee, S.-Y., Varghese, V., Porter, D., White, K., Taylor, J., Towner, W., Troia, P., Burack, J., Dejesus, E., et al. 2014. *Non-nucleoside reverse transcriptase inhibitor (NNRTI) cross-resistance: implications for preclinical evaluation of novel*

*NNRTIs and clinical genotypic resistance testing.* The Journal of antimicrobial chemotherapy 69(1):12–20.

Mitsuya, H., Weinhold, K. J., Furman, P. A., St Clair, M. H., Lehrman, S. N., Gallo, R. C., Bolognesi, D., Barry, D. W., & Broder, S. 1985. *3'-Azido-3'-deoxythymidine (BW A509U): an antiviral agent that inhibits the infectivity and cytopathic effect of human T-lymphotropic virus type III/lymphadenopathy-associated virus in vitro.* Proceedings of the National Academy of Sciences of the United States of America 82(20):7096–7100.

Morris, G. M., Huey, R., Lindstrom, W., Sanner, M. F., Belew, R. K., Goodsell, D. S., & Olson, A. J. 2009. *AutoDock4 and AutoDockTools4: Automated docking with selective receptor flexibility.* Journal of computational chemistry 30(16):2785–91.

Rathwell, D. C. K., Yang, S.-H., Tsang, K. Y., & Brimble, M. A. 2009. *An efficient formal synthesis of the human telomerase inhibitor (+/-)-gamma-rubromycin.* Angewandte Chemie (International ed. in English) 48(43):7996–8000.

Reuman, E. C., Rhee, S.-Y., Holmes, S. P., & Shafer, R. W. 2010. *Constrained patterns of covariation and clustering of HIV-1 non-nucleoside reverse transcriptase inhibitor resistance mutations.* The Journal of antimicrobial chemotherapy 65(7):1477–85.

Rhee, S.-Y., Liu, T., Ravela, J., Gonzales, M. J., & Shafer, R. W. 2004. *Distribution of human immunodeficiency virus type 1 protease and reverse transcriptase mutation patterns in 4,183 persons undergoing genotypic resistance testing.* Antimicrobial agents and chemotherapy 48(8):3122–6.

Rimsky, L., Vingerhoets, J., Van Eygen, V., Eron, J., Clotet, B., Hoogstoel, A., Boven, K., & Picchio, G. 2012. *Genotypic and phenotypic characterization of HIV-1 isolates obtained from patients on rilpivirine therapy experiencing virologic failure in the phase 3 ECHO and THRIVE studies: 48-week analysis.* Journal of acquired immune deficiency syndromes (1999) 59(1):39–46.

Sarafianos, S. G., Marchand, B., Das, K., Himmel, D. M., Parniak, M. a, Hughes, S. H., & Arnold, E. 2009. *Structure and function of HIV-1 reverse transcriptase: molecular mechanisms of polymerization and inhibition.* Journal of molecular biology 385(3):693–713.

Singh, K., Marchand, B., Kirby, K. a, Michailidis, E., & Sarafianos, S. G. 2010. *Structural Aspects of Drug Resistance and Inhibition of HIV-1 Reverse Transcriptase.* Viruses 2(2):606–638.

Singh, K., Marchand, B., Rai, D. K., Sharma, B., Michailidis, E., Ryan, E. M., Matzek, K. B., Leslie, M. D., Hagedorn, A. N., Li, Z., et al. 2012. *Biochemical mechanism of HIV-1 resistance to rilpivirine.* The Journal of biological chemistry 287(45):38110–38123.

Srinivasan, J., Cheatham, T. E., Cieplak, P., Kollman, P. A., & Case, D. A. 1998. *Continuum Solvent Studies of the Stability of DNA , RNA , and Phosphoramidate - DNA Helices* 7863(98).

Tambuyzer, L., Vingerhoets, J., Azijn, H., Daems, B., Nijs, S., de Béthune, M.-P., & Picchio, G. 2010. *Characterization of genotypic and phenotypic changes in HIV-1-infected patients with virologic failure on an etravirine-containing regimen in the DUET-1 and DUET-2 clinical studies*. *AIDS research and human retroviruses* 26(11):1197–205.

Ueno, T., Takahashi, H., Oda, M., Mizunuma, M., Yokoyama, A., Goto, Y., Mizushima, Y., Sakaguchi, K., & Hayashi, H. 2000. *Inhibition of Human Telomerase by Rubromycins: Implication of Spiroketal System of the Compounds as an Active Moiety*. *Biochemistry* 39(20):5995–6002.

Wang, J., Morin, P., Wang, W., & Kollman, P. A. 2001. *Use of MM-PBSA in Reproducing the Binding Free Energies to HIV-1 RT of TIBO Derivatives and Predicting the Binding Mode to HIV-1 RT of Efavirenz by Docking and MM-PBSA*. *Journal of the American Chemical Society* 123(22):5221–5230.

Wu, K.-L., Mercado, E. V., & Pettus, T. R. R. 2011. *A convergent total synthesis of (±)- $\gamma$ -rubromycin*. *Journal of the American Chemical Society* 133(16):6114–7.

Yuen, T.-Y., Ng, Y.-P., Ip, F. C. F., Chen, J. L.-Y., Atkinson, D. J., Sperry, J., Ip, N. Y., & Brimble, M. a. 2013. *Telomerase Inhibition Studies of Novel Spiroketal-Containing Rubromycin Derivatives*. *Australian Journal of Chemistry* 530–533.

Zhang, Z., Xu, W., Koh, Y.-H., Shim, J. H., Girardet, J.-L., Yeh, L.-T., Hamatake, R. K., & Hong, Z. 2007. *A novel nonnucleoside analogue that inhibits human immunodeficiency virus type 1 isolates resistant to current nonnucleoside reverse transcriptase inhibitors*. *Antimicrobial agents and chemotherapy* 51(2):429–37.